Effects of Deck Shape and Oncoming Turbulence on Bridge Aerodynamics

Yuh-Yi Lin*, Chii-Ming Cheng, Jong-Cheng Wu, Tsang-Lien Lan and Kuo-Ting Wu

Department of Civil Engineering, Tamkang University, Tamsui, Taiwan 251, R.O.C.

Abstract

The influence of deck geometry and oncoming turbulence on the flutter and buffeting behavior of cable-supported bridges were investigated by using wind tunnel section model test. In addition to smooth flow, homogeneous turbulent flow fields with various intensities and integral scales were generated for the aerodynamic coefficient measurements. The flutter wind speed and buffeting dynamic response were evaluated by incorporating the measured aerodynamic coefficients into the analytical model of a cable-stayed bridge. The results show that the width-to-depth ratio, B/H, of bridge deck plays an important role in bridge aerodynamics. Increasing B/H will improve the bridge stability. This study also indicates that the critical flutter wind speed increases monotonically with turbulence intensity, in other words, free stream turbulence tends to enhance the bridge's aerodynamic stability. Using the wind force coefficients and flutter derivatives obtained from smooth flow condition may result in larger buffeting estimation than those obtained from turbulent flows. These calculated results coincide reasonably with the measured results.

***Key Words*:** Deck Shape, Turbulence, Section Model, Bridge

1. Introduction

The development of advanced high strength materials and bridge construction techniques make cable-stayed bridge a suitable choice for long span crossing. In many places such as Taiwan, the special aesthetic impression and the high visibility put cable-stayed bridge among the favorable choices of bridge types, sometimes overruling the economic considerations. Because of the lightweight and the flexibility nature of this bridge type, long span cable-stayed bridges are more vulnerable to aerodynamic instability. The most important aerodynamic phenomenon can be categorized as: (a) aerodynamic instability - torsional divergence (static) and flutter (dynamic); (b) buffeting and vortex shedding due to approaching flow.

Bridge aerodynamics, in its early stage, was spin-off aerospace study. Scanlan and Tomko [1] are the pioneers who modified Theodorsen's flutter theory and then applied it to the bluff-body shaped long span bridges. Instead of using the analytical airfoil formulation, experimental approach was adopted to obtain the flutter derivatives for the bluff body bridge decks. Three types of bridge model tests, i.e., full model, section model, and taut-strip model, are currently being used in wind tunnel test to study the aerodynamic characteristics of the cable-supported bridges. Among them, section model is commonly used for the identification of bridge aerodynamic parameters.

Generally speaking, bridge aerodynamic phenomenon is the results of wind-structure interaction. It has been established by many researchers that the characteristics of bridge's aerodynamic stability is under the influence of several factors: structural natural frequencies, frequency ratio, deck geometry and wind conditions. Bienkiewicz [2] studied section model of different cross

*Corresponding author. E-mail: yyl@mail.tku.edu.tw

sections and Nagao et al. [3] studied box girder with two B/H ratios and different forms of fairing. In these studies they concluded that the better streamlined deck cross section leads to better bridge aerodynamic stability. Investigations conducted by Matsumoto and his associates [4,5] on plate section with various B/H ratios indicated that the bridge deck with smaller B/H ratio is less aerodynamically stable and tends to result in the single-degree-of-freedom flutter. As for the effects of turbulence on bridge stability, Scanlan and Lin [6] and Huston et al. [7] studied the flutter derivatives of section model and then concluded that turbulence has insignificant influence on bridge flutter. However, Wardlaw et al. [8] found that turbulence can suppress the vortex shedding and buffeting responses.

This paper intends to study the effects of deck shape and oncoming turbulence on bridge flutter and buffeting characteristics. Two basic deck sections-closed box girder and plate girder-each with various B/H ratios were tested in smooth and turbulent flow fields. The static wind force coefficients and the flutter derivatives were measured in these wind tunnel tests. Based on the measured aerodynamic coefficients, bridge's flutter wind speed and buffeting response were then analyzed. The calculated results were compared with the measured section model responses reported in the authors' another paper [9].

2. Flutter and Buffeting Analysis

Consider a 2-DOF section model of bridge deck subjected to turbulent oncoming flow. Fluctuating wind loads that act on the deck can be represented by a combination of a motion-induced self-excited force and a buffeting force. The equations of motion in the drag, lift (heave) and torsional (pitch) directions are expressed as [1]:

$$m_x(\ddot{x} + 2\xi_x\omega_x\dot{x} + \omega_x^2 x) = D_f + D_b \tag{1}$$

$$m_y(\ddot{y} + 2\xi_y\omega_y\dot{y} + \omega_y^2 y) = L_f + L_b \tag{2}$$

$$I(\ddot{\alpha} + 2\xi_\alpha\omega_\alpha\dot{\alpha} + \omega_\alpha^2\alpha) = M_f + M_b \tag{3}$$

in which the subscript f and b are self-excited force and turbulence induced buffeting force, respectively. The linearized form of the self-excited force can be written as:

$$D_f(t) = \frac{1}{2}\rho U^2(2B)(K) \times \left[P_1^*(K)\frac{\dot{z}(t)}{U} + P_2^*(K)\frac{B\dot{\alpha}(t)}{U} + KP_3^*(K)\alpha(t)\right] \tag{4}$$

$$L_f(t) = \frac{1}{2}\rho U^2(2B)(K) \times \left[H_1^*(K)\frac{\dot{y}(t)}{U} + H_2^*(K)\frac{B\dot{\alpha}(t)}{U} + KH_3^*(K)\alpha(t)\right] \tag{5}$$

$$M_f(t) = \frac{1}{2}\rho U^2(2B^2)(K) \times \left[A_1^*(K)\frac{\dot{y}(t)}{U} + A_2^*(K)\frac{B\dot{\alpha}(t)}{U} + KA_3^*(K)\alpha(t)\right] \tag{6}$$

where $K = \frac{B\omega}{U}$ is reduced frequency, ω is the circular frequency, B is the deck width, ρ is air density, U is average wind speed, y, z, α represent drag, lift and torsional displacements, respectively. $H_j^*(K)$, $P_j^*(K)$, $A_j^*(K)$ $(j = 1,3)$ are non-dimensional aerodynamic coefficients, called flutter derivatives, which represent certain aeroelastic phenomenon induced by wind-structure interaction. The flutter derivatives are functions of deck geometry, reduced frequency and flow field, the first two factors cast most of the influence on them.

The buffeting forces on a bridge deck section in the drag, vertical, and torsional directions can be simplified as follows:

$$D_b(t) = \frac{1}{2}\rho U^2 BC_D(\alpha_0)\left(\frac{2u}{U}\right) \tag{7}$$

$$L_b(t) = \frac{1}{2}\rho U^2 B\left\{C_L(\alpha_0)\frac{2u}{U} + \left[\left.\frac{dC_L}{d\alpha}\right|_{\alpha=\alpha_0} + C_D(\alpha_0)\right]\frac{w}{U}\right\} \tag{8}$$

$$M_b(t) = \frac{1}{2}\rho U^2 B^2 \times \left\{\left[C_M(\alpha_0) + C_D(\alpha_0)\frac{Ar}{B^2}\right]\frac{2u}{U} + \left.\frac{dC_M}{d\alpha}\right|_{\alpha=\alpha_0}\frac{w}{U}\right\} \tag{9}$$

in which b represents buffeting effect, u, w are velocity fluctuations in the drag and lift directions, C_D, C_L, C_M are the drag, lift and torstional wind force coefficients, α_0 is mean wind angle of attack, A is the deck's projected area on the vertical axis, and r is the distance of deck mass center from the effective axis of rotation.

Substituting the empirical flutter derivatives into Eqs. (4)–(6), the self-excited forces can be found. Then substituting the self-excited forces into deck equations of motion, Eqs. (1)–(3), the aerodynamic stiffness and aerodynamic damping effects are incorporated with the structural system. The system natural frequency and critical velocity for onset of flutter can be found by using the complex eigen-value analysis. As for the bridge's buffeting response, the mechanic admittance for the structural system and the aerodynamic effects are put to use with spectra for various wind speed fluctuations [10]. The dynamic responses can be obtained through a simple spectral analysis. A unit admittance function is assumed in this analysis. The spectra and cross-spectra of horizontal and vertical wind speed fluctuations used in this study are stated as follows [11]:

For the spectrum of horizontal wind speed fluctuations

$$S_u(n) = \frac{200\frac{z}{U}u_*^2}{\left(1+50\frac{nz}{U}\right)^{5/3}} \tag{10}$$

For the spectrum of vertical wind speed fluctuations

$$S_w(n) = \frac{3.36\frac{z}{U}u_*^2}{1+10\left(\frac{nz}{U}\right)^{5/3}} \tag{11}$$

For the cross-spectrum of horizontal and vertical wind speed fluctuations

$$S_{r_i r_j}^{C}(n) = S_r(n)\exp\left[-\frac{C_r n\left|x_i - x_j\right|}{U}\right];\ (\mathrm{r} = \mathrm{u},\ \mathrm{w}) \tag{12}$$

where n is frequency; u_* is the friction velocity; z is the height above ground; C_r is the empirical constants, 16 and 8 are used for the horizontal and vertical wind speed fluctuations, respectively; x_i and x_j are the longitudinal coordinates of nodes i and j, respectively.

A cable-stayed bridge with a major span of 720 m and two side spans, each of 220 m, is used for the flutter and buffeting analysis. A finite element model, consisting of beam-column elements and cable elements, is used to model the bridge deck, tower, and cables in the structural analysis. The geometry of the bridge and the general view of the deck cross sections are shown in Figures 1 and 2. The structural properties and the vibration mode characteristics of the bridge are listed in Tables 1 and 2. Only the first lift mode and torsional mode were used in the flutter analysis. As for the buffeting analysis, the first ten structural modes were included.

3. Experimental Apparatus

The section model test was conducted in the Bound-

Table 1. Sectional properties of the prototype

Properties \ Model	Prototype
Width (m)	35 (20 for model 2)
Mass (kg/m)	25400
Polar mass moment of inertia (kg-m^2/m)	3,600,000
Vertical frequency (Hz)	0.167
Torsional frequency (Hz)	0.368
Torsional-to-vertical frequency ratio	2.2

Table 2. First 10 structural modes of the cable-stayed bridge

Mode	Frequency (Hz)	Dominant axis	Mode	Frequency (Hz)	Dominant axis
1	0.167	Lift	6	0.439	Lift
2	0.174	Drag	7	0.488	Drag
3	0.229	Lift	8	0.494	Tower
4	0.348	Lift	9	0.497	Lift
5	0.368	Torsional	10	0.5	Drag

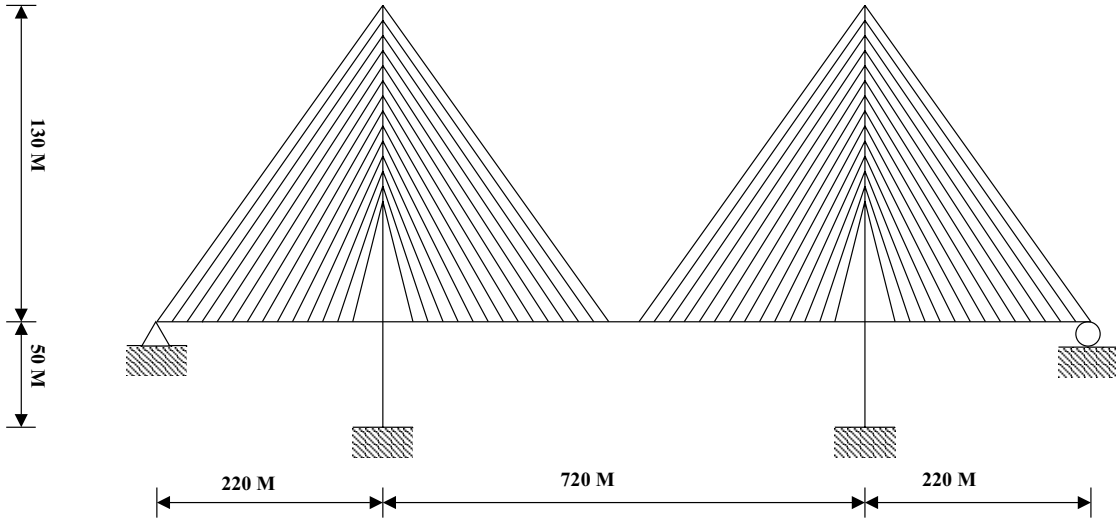

Figure 1. Geometry of the prototype bridge.

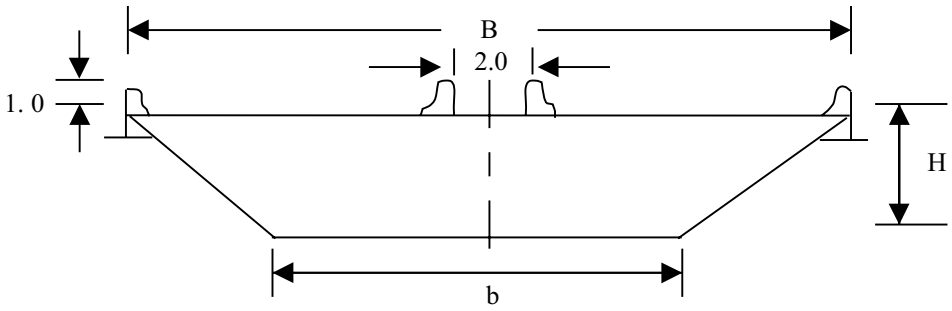

Model	1–1	1–2	1–3	1–4
H(cm)	1.75	2.4	3.2	5
b(cm)	27.7	25.4	21.8	15.4

(closed box girder)

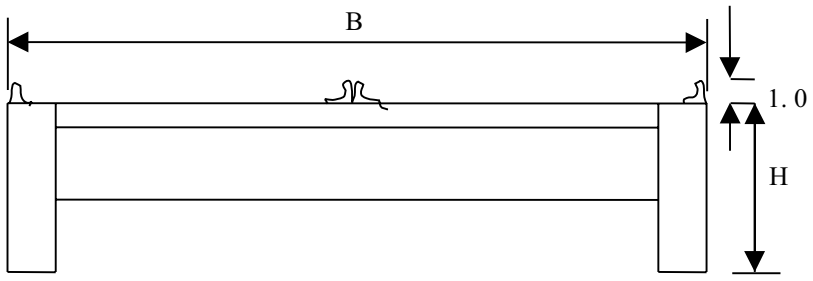

Model	2–1	2–2	2–3	2–4
H(cm)	1.5	2	3	5

(plate girder)

Figure 2. Geometry of section models.

ary Layer Wind Tunnel in Tamkang University. The wind tunnel has a working section of 3.2 m(W) × 2.0 m(H) × 18.7 m(L). The bridge deck model of 1.5 m was placed between two end plates in the test. Two controlling parameters were selected-the B/H ratio and the oncoming turbulence. Two types of decks, one of the box girder type (model 1 series) and the other of the plate girder type (model 2 series), were selected to investigate the effects of B/H ratios on bridge aerodynamics. For each type of deck, four section models, with B/H ratios from 4 to 20, were built and tested. The geometry of these decks is shown in Figure 2 and the B/H ratios are shown in Table 3. In this part of study, all eight models were tested under smooth flow and zero wind attack angle condition.

In the second phase of this study, the authors investigated the influence of turbulence on bridge aerodynamic behavior. Two sets of grids were used to generate homogeneous turbulent flow fields for model testing. By changing the distance between the grids and the section model, five turbulent flow fields were generated. The turbulence intensity varies from 1% in the smooth flow up to 16% in the flow field E. Flow conditions and the turbulence length scale L_u are listed in Table 4. For this part of study, only model 1–3 (B/H = 11) and model 2–3 (B/H = 6.7) were used for wind tunnel testing.

In each of the test cases, wind force coefficients, C_D, C_L, C_M, and flutter derivatives, H_j^*, A_j^* (j = 1,3), were measured. Force coefficients were measured when the bridge section model was stationary. For the identification of flutter derivatives, section model was arranged in such a way that it could be either in a pure torsional motion or in a coupled mode motion. The measured aerodynamic coefficients were then substituted into the analytical model for the subsequent bridge flutter and buffeting analysis.

4. Experimental Measurements

4.1 Force Coefficients

The force coefficients of section models measured in smooth flow are shown in Figures. 3–4. It shows that, for both model series 1 and 2, as the section model's B/H ratio increases, drag coefficient (normalized w.r.t a constant bridge width) decreases due to the smaller front projected area. The B/H ratio makes only slight differences on the lift coefficient of the closed box girder (model series 1). The absolute value of C_L decreases significantly when the B/H ratio of the plate girder (model series 2) decreases. In the case of the model 2–4, the relationship between the lift coefficient and attack angle is quite different from those of the other three models. As for the torsional moment coefficient C_M, it increases with model's B/H ratio in model series 1. However, for the plate girder, a thicker deck (with smaller B/H) is subjected to a smaller torque at negative wind attack angle, but a larger torque at positive wind attack angle. It is worth to mention that the torsional moment coefficient of the model 2–4 is significantly larger than those of the other three models at zero angle of attack. The influence of the oncoming turbulence on the force coefficients, shown in Figures 5 and 6, are similar for both the closed box girder and the plate girder bridge decks. Higher free stream turbulence tends to enhance the reattachment and weaken the wake formation, and therefore, reduce the wind loads on all three directions. Larger wind attack angle amplifies the turbulence effect. Although the higher turbulence induces larger fluctuating wind load, the smooth flow condition tends to make bridge deck have larger force coefficients which in turn will produce larger bridge's dynamic response during the analytical buffeting calculation.

Table 4. Properties of turbulent flows

Flow field	S	A	B	C	D	E
Turbulence intensity (%)	1	5	8	11	14	16
Length scale ratio *(L_U/H)*	--	4	4	8	8	8

Table 3. Geometry of section models

Deck shape	Closed box girder (model 1 series)				Plate girder (model 2 series)			
Model	1–1	1–2	1–3	1–4	2–1	2–2	2–3	2–4
B/H	20	14.6	11	7	13.3	10	6.7	4

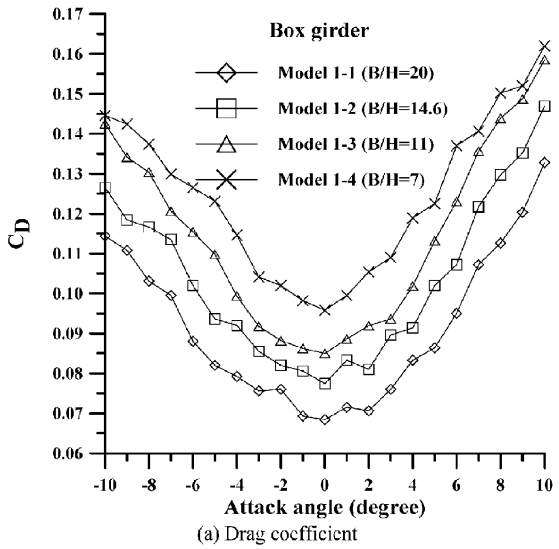

(a) Drag coefficient

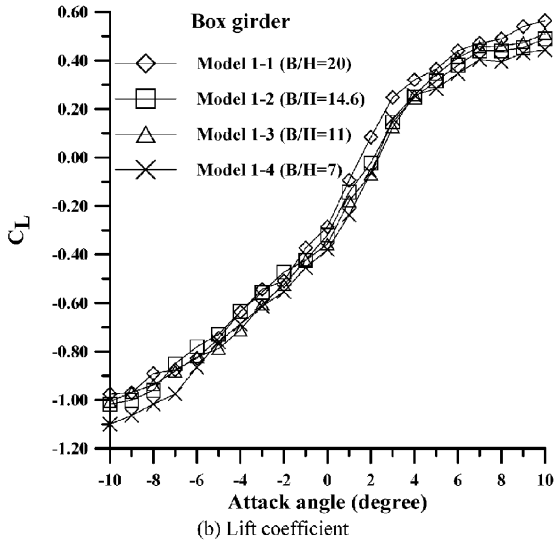

(b) Lift coefficient

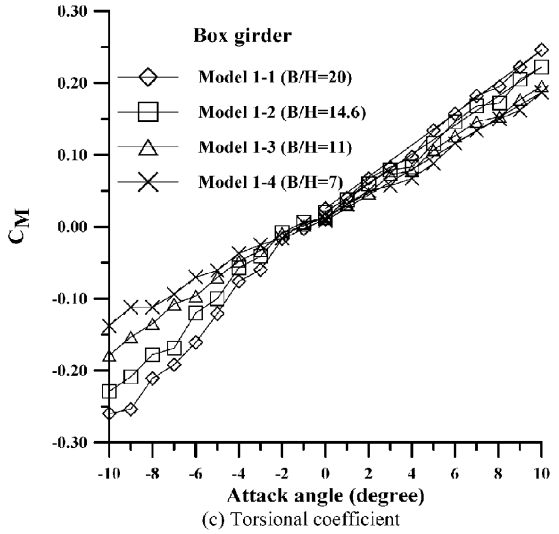

(c) Torsional coefficient

Figure 3. Effects of deck shape on force coefficient-box girder (a) drag coefficient (b) lift coefficient (c) torsional coefficient.

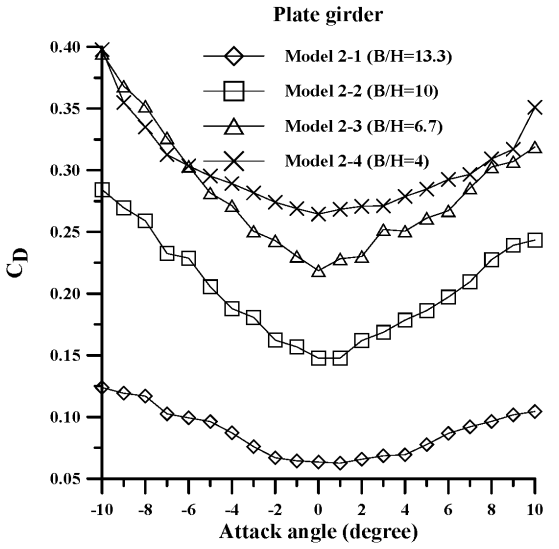

(a) Drag coefficient

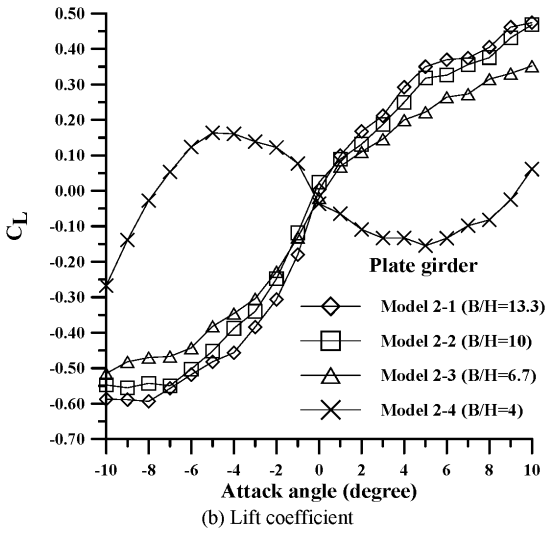

(b) Lift coefficient

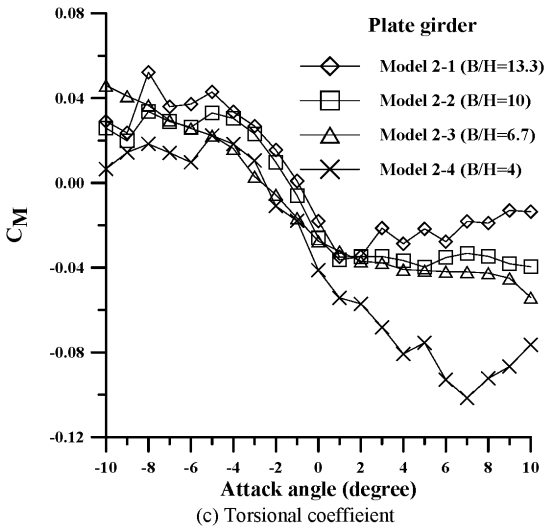

(c) Torsional coeffieient

Figure 4. Effects of deck shape on force coefficient-plate girder (a) drag coefficient (b) lift coefficient (c) torsional coefficient.

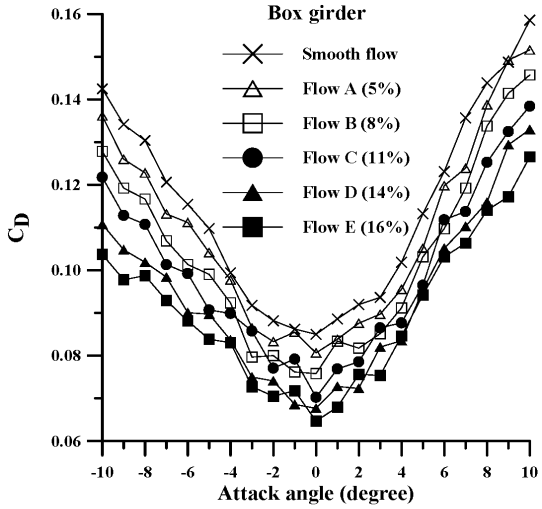

(a) Drag coefficient

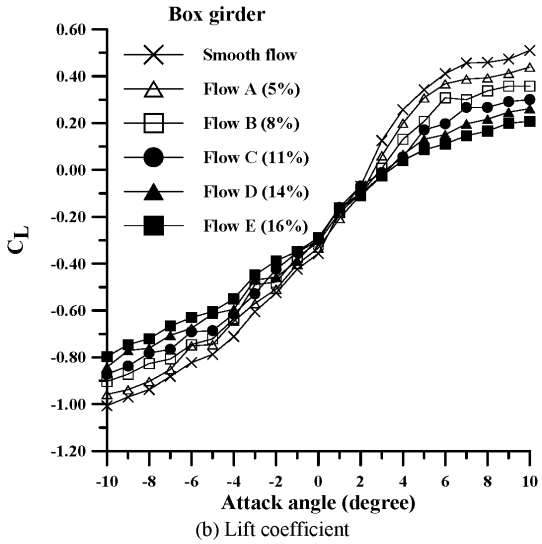

(b) Lift coefficient

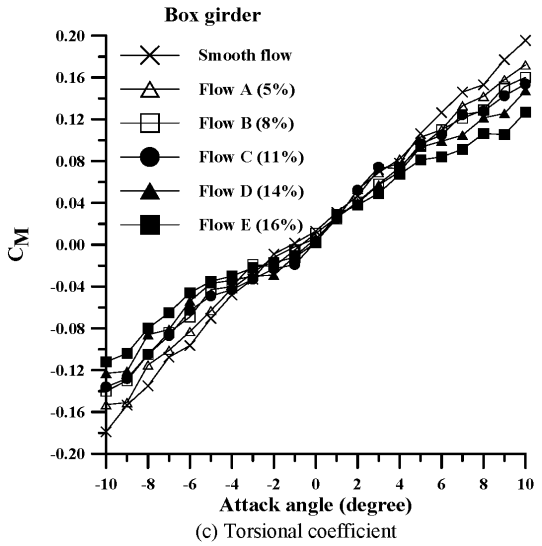

(c) Torsional coefficient

Figure 5. Turbulence effects on force coefficients of model 1–3.

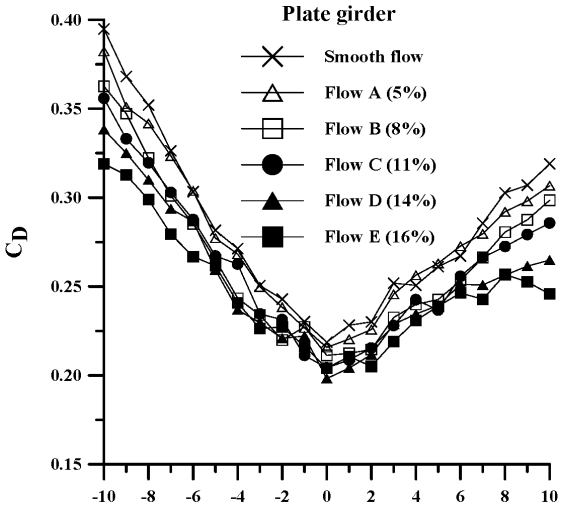

(a) Drag coefficient

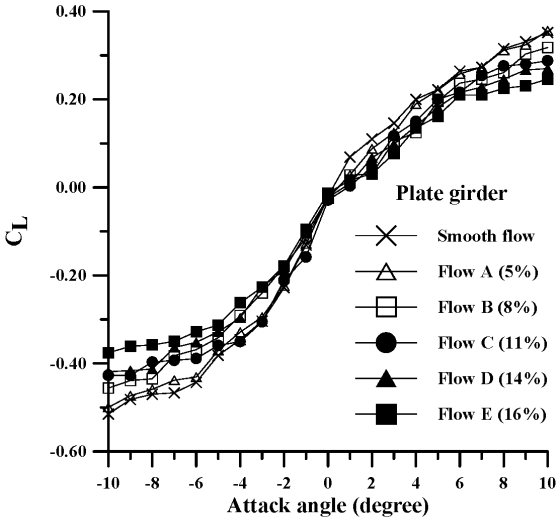

(b) Lift coefficient

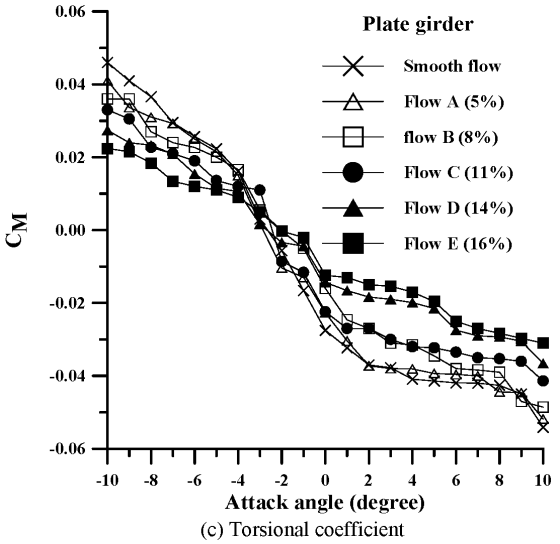

(c) Torsional coefficient

Figure 6. Turbulence effects on force coefficients of model 2–3.

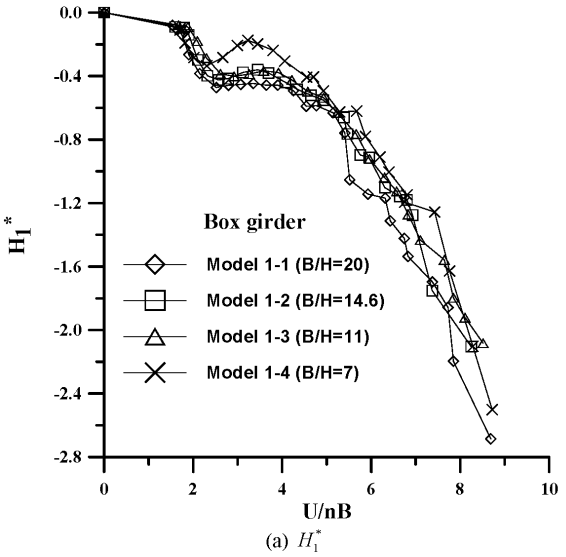

(a) H_1^*

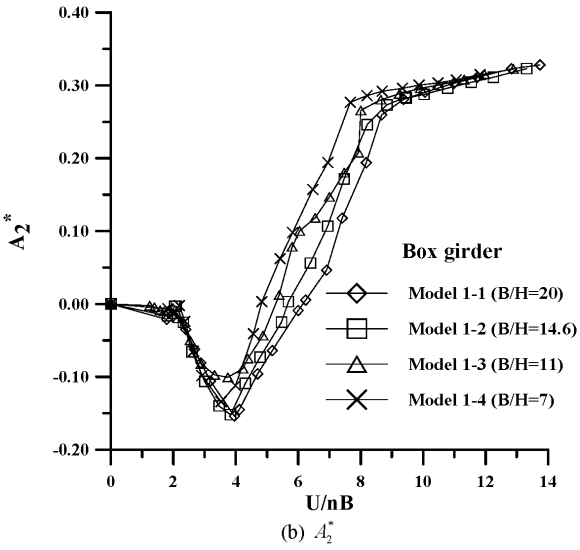

(b) A_2^*

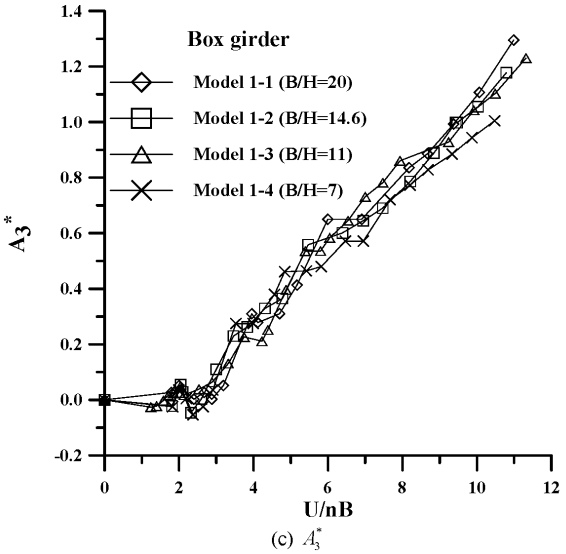

(c) A_3^*

Figure 7. Effects of deck shape on flutter derivatives-box girder (a) H_1^* (b) A_2^* (c) A_3^*.

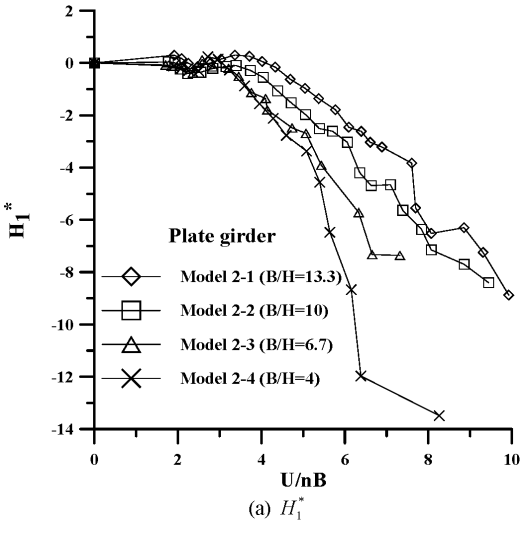

(a) H_1^*

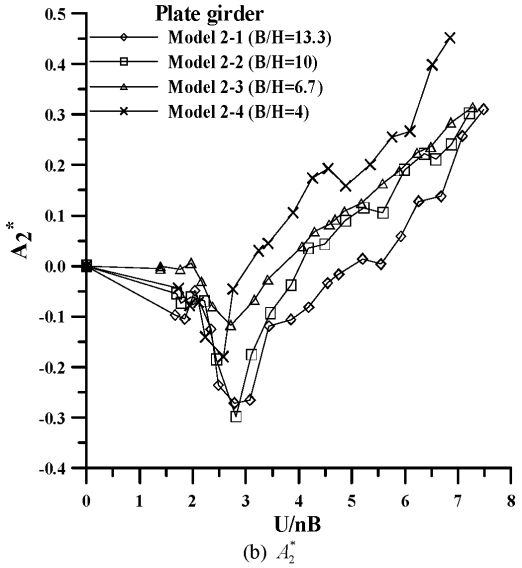

(b) A_2^*

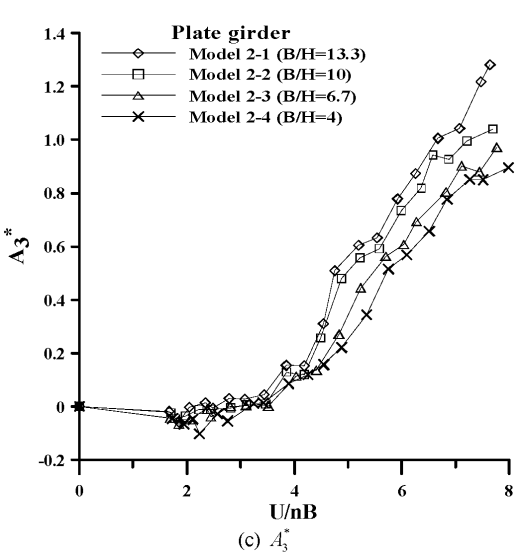

(c) A_3^*

Figure 8. Effects of deck shape on flutter derivatives-plate girder (a) H_1^* (b) A_2^* (c) A_3^*.

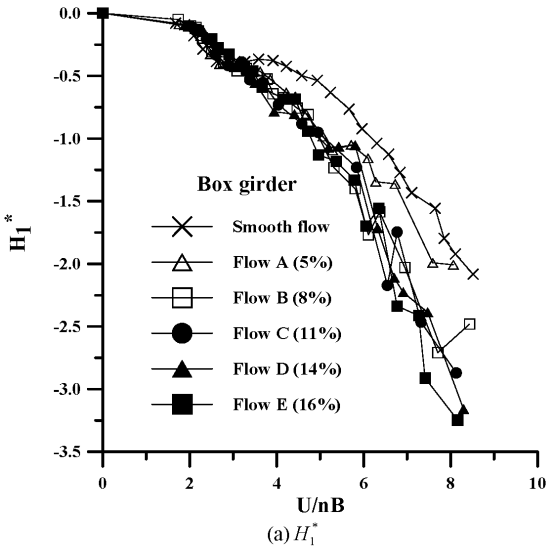

(a) H_1^*

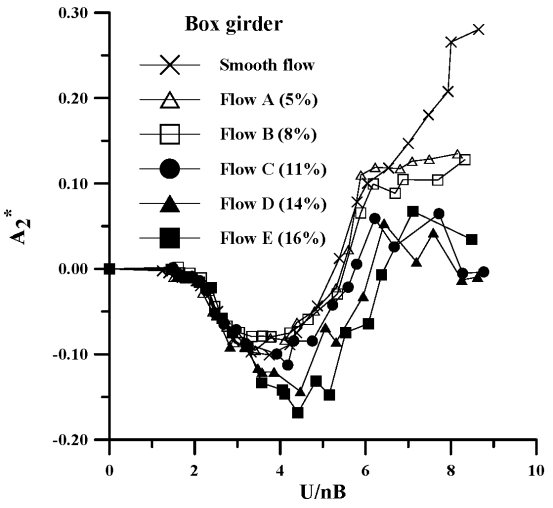

(b) A_2^*

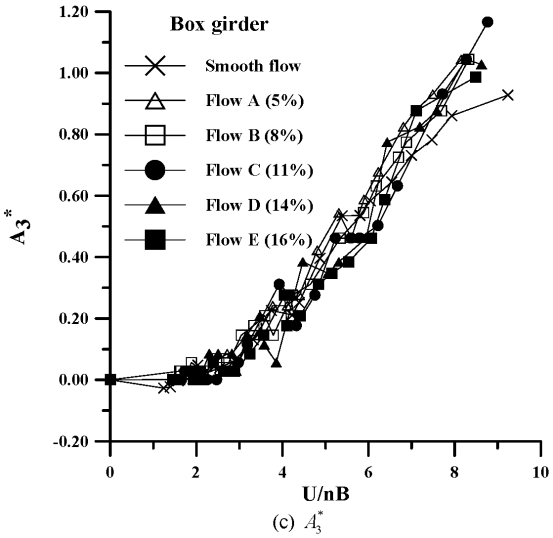

(c) A_3^*

Figure 9. Turbulence effect on flutter derivatives of model 1–3 (a) H_1^* (b) A_2^* (c) A_3^*.

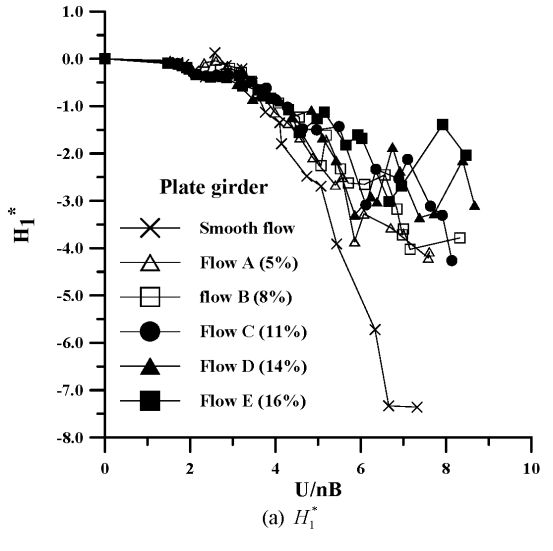

(a) H_1^*

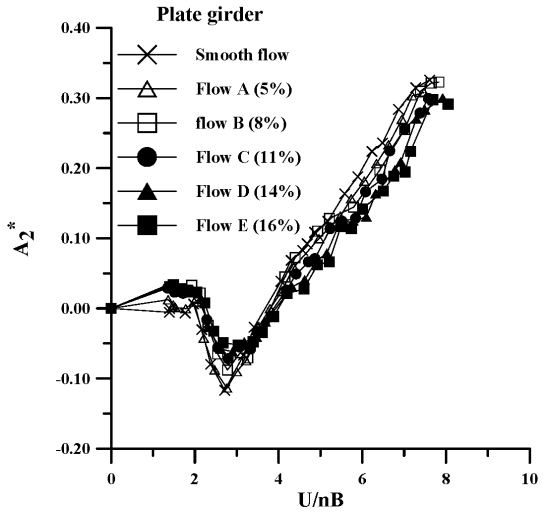

(b) A_2^*

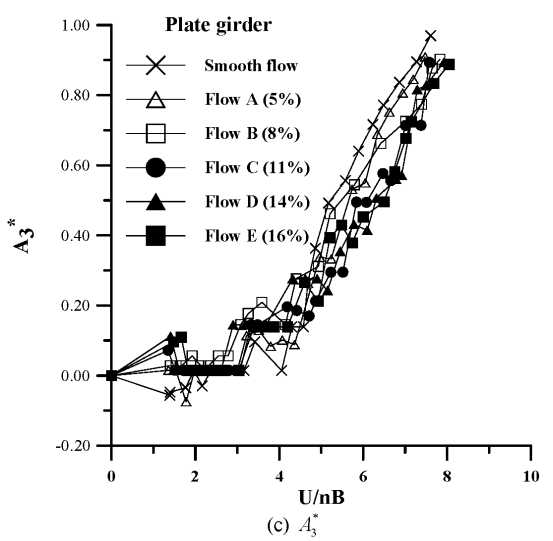

(c) A_3^*

Figure 10. Turbulence effect on flutter derivatives of model 2–3 (a) H_1^* (b) A_2^* (c) A_3^*.

4.2 Flutter Derivatives

The uncoupled flutter derivatives (H_1^*, A_2^*, A_3^*) of all section models tested in smooth flow are shown in Figures 7 and 8. Both model series 1 and 2 have negative values of H_1^* which indicates a positive aerodynamic damping effect on the lift vibration mode. The plate girder models in general have larger absolute values of H_1^* than the closed box girder model. It also can be found that the plate girder shows a more distinctive trend of H_1^* with B/H ratio than the closed box girder. Except at very low reduced velocities, both model series 1 and 2 exhibit positive value of A_3^* which represents a negative torsional aerodynamic stiffness effect. Model series 1 has a slightly higher A_3^* than series 2, which suggests that model series 1 is more likely to exhibit coupled-mode motion. For this flutter derivative, the B/H ratio does not cast significant effect on model series 1, while it does on model series 2. The value of A_3^* of the plate girder increases with the B/H ratio. A_2^*, which represents the torsional aerodynamic damping effect, is the most important flutter derivative on bridge aerodynamic stability. Both types of models show negative A_2^* at low reduced velocities and positive value of A_2^* at high reduced velocities. For the closed box girders, A_2^* becomes positive at wind speeds Ur = 4.5–6.5. In the cases of plate girder models, sign change on A_2^* occurs at earlier wind speeds, Ur = 3–5.5. This indicates that the plate girder model tends to show negative aerodynamic damping in the torsional mode at a lower wind speed than the closed box girder. The results imply that the plate girder is a less stable bridge cross section. Also, it can be found that the increase of B/H ratio will delay the occurrence of negative torsional aerodynamic damping for both types of bridge decks.

Figures 9 and 10 show the flutter derivatives of model 1–3 and 2–3 measured at various flow fields. For the closed box girder 1–3, turbulence tends to increase the absolute value of H_1^*, i.e., increase the positive aerodynamic damping in the vertical direction. However, the flat plate girder 2–3 has a reverse effect; the higher the turbulence intensity, the lower the absolute value of H_1^*. As for the torsional aerodynamic damping, the reduced wind speed corresponding to the sign change of A_2^* increases with turbulence intensity in both models. It shows that turbulence tends to make bridges more aerodynamically stable. The effect of turbulence on flutter derivative A_3^* is indistinct on model 1–3, but on model 2–3. It can be observed that A_3^* decreases as turbulence intensity increases.

5. Bridge's Critical Flutter Wind Speed

The critical flutter wind speeds were evaluated by substituting the flutter derivatives into the numerical model, for both single-degree-of-freedom flutter and coupled flutter analyses. Detailed analytical procedure is described in the reference [10]. Table 5 indicates that bridge model series 1, which was more streamlined, has significantly higher flutter wind speeds than model series 2. When B/H ratio of model series 1 varies from 7 to 20, the flutter wind speed increases by 1520%. For model series 2, the change of B/H ratio from 4 to 13, the increase of the flutter wind speed can be more than 50%. In other words, selecting a flatter deck shape can improve bridge aerodynamic stability. This phenomenon is more effective for a "bluff body like" deck than a

Table 5. Flutter wind speeds and flutter frequencies for various model shapes

Model	Flutter wind speed (m/s)			Flutter frequency (Hz)	
	Uncoupled	Coupled	Measured	Uncoupled	Coupled
1–1	72	69.1	60.9	0.322	0.3244
1–2	66.2	63.9	59.7	0.326	0.3272
1–3	62.8	59.8	59.2	0.324	0.328
1–4	57	55.5	55.2	0.332	0.3359
2–1	45.5	45	42.3	0.365	0.365
2–2	41.9	37.8	39.6	0.367	0.367
2–3	36.9	36.7	36.3	0.367	0.367
2–4	29.2	29.2	29.4	0.369	0.368

more "streamlined like" deck. Table 5 lists the flutter wind speeds based on both the aerodynamically coupled and uncoupled analyses. For model series 1, the flutter wind speed based on the coupled mode analysis is slightly lower than the one from the uncoupled analysis. The little difference between two methods is due to the fact that the frequency ratio of the first torsional mode to the first lift mode of the prototype bridge is 2.2, which will not induce significant mode coupling. As for the model series 2, there is virtually no difference between coupled and uncoupled flutter analyses. In short, the plate girder deck tends to flutter in a single-degree-of-freedom mode, whereas the box girder deck tends to flutter in coupled modes. The results in Table 5 also indicate that the calculated flutter wind speeds are in good agreement with the measured results reported in reference [9].

The flutter wind speeds of both model 13 and 23 were calculated for different flow fields, as listed in Table 6. For both bridge deck models under study, the critical flutter wind speed increases monotonically with turbulence intensity. Regardless of the geometric shape of bridge deck, free stream turbulence tends to enhance the bridge's aerodynamic stability. For comparison, the measured results obtained from reference [9] are also included. From the comparison of the results, it can be seen that the calculated results in this study are consistent with the measured results. Although there is some discrepancy found in model 2, the difference is not significant.

Table 6. Flutter wind speeds at various flow fields

Flow fields	Model 1–3			Model 2–3		
	Calculated flutter wind speed (m/s)	Calculated flutter frequency (Hz)	Measured flutter wind speed (m/s)	Calculated flutter wind speed (m/s)	Calculated flutter frequency (Hz)	Measured flutter wind speed (m/s)
S	59.8	0.328	59.2	36.7	0.367	36.3
A	61.5	0.330	60.7	38.2	0.365	42.3
B	62.7	0.331	61.4	36.7	0.365	43.5
C	65.4	0.318	63.03	38.8	0.365	43.2
D	69.2	0.329	–	39.6	0.365	–
E	67.3	0.326	63.7	42	0.364	46.2

Table 7. Maximum RMS buffeting responses of Model 1 at 50 m/s (Ti = 10%)

Model 1	Drag (m)	Lift (m)		Torsional (degree)	
		Calculated	Measured	Calculated	Measured
1–1	0.04994	0.811	1.057	0.5316	0.582
1–2	0.05525	0.8018	0.937	0.5139	0.556
1–3	0.05921	0.766	0.897	0.4629	0.52
1–4	0.06624	0.6585	0.863	0.5181	0.468

Table 8. Maximum RMS buffeting responses of Model 2 at 35 m/s (Ti = 10%)

Model 2	Drag (m)	Lift (m)		Torsional (degree)	
		Calculated	Measured	Calculated	Measured
2–1	0.01	0.32	0.459	0.1133	0.196
2–2	0.02314	0.244	0.355	0.2165	0.181
2–3	0.0307	0.18	0.281	0.234	0.245
2–4*	0.0237	0.11	0.167	0.34	0.438

* Results were calculated and measured at 28 m/s.

Table 9. Maximum RMS buffeting responses of Model 1–3 at 50 m/s

Flow field	Lift (m)			Torsional (degree)		
	Calculated		Measured	Calculated		Measured
	S*	T**		S*	T**	
A	0.3743	0.29	0.165	0.228	0.2023	0.1775
B	0.625	0.448	0.595	0.38	0.308	0.478
C	0.876	0.658	0.897	0.529	0.429	0.52
D	1.092	0.76	1.545	0.660	0.554	0.957
E	1.256	0.837	1.745	0.759	0.622	1.189

*Use the coefficients measured in smooth flow; **Use the coefficients measured in turbulent flow.

Table 10. Maximum RMS buffeting responses of Model 2–3 at 35 m/s

Flow field	Lift (m)			Torsional (degree)		
	Calculated		Measured	Calculated		Measured
	S*	T**		S*	T**	
A	0.083	0.077	0.12	0.1	0.064	0.108
B	0.136	0.12	0.19	0.17	0.15	0.17
C	0.189	0.215	0.254	0.23	0.144	0.193
D	0.236	0.194	0.343	0.287	0.185	0.295
E	0.2717	0.261	0.38	0.33	0.225	0.323

*Use the coefficients measured in smooth flow; **Use the coefficients measured in turbulent flow.

6. Bridge's Buffeting Response

The buffeting responses were calculated assuming that the prototype bridge is subjected to the turbulent wind with the turbulence intensity of 10%. The wind force coefficients and the flutter derivatives of the decks used in the calculation were measured in smooth flow. Using the buffeting theory, the maximum RMS responses of bridge decks with model 1 and model 2 are respectively calculated at wind speed of 50 *m/s* and 35 *m/s*. The results are listed in Table 7 and Table 8, respectively. The measured results obtained from reference [9] are also included in these tables. It should be pointed out that the two series of bridge models have different widths and assumed under the same scaling ratio. In other words, the prototype bridges also have two different widths, therefore, the responses should not be compared between the two types of bridges. The data listed in Tables 7 and 8 indicates that, although the effects of structural mode coupling and bridge aeroelastic effects are included in the buffeting analysis, the bridge dynamic responses basically follow the same trend as the corresponding force coefficients. For example, the lift and torsional RMS responses of model series 1 increase with B/H ratio. These trends coincide with the variation of the corresponding force coefficients. The drag buffeting responses of model series 1 and 2 increase as the B/H ratio decreases. These results can be expected because the deck with the smaller B/H ratio has the larger depth and results in the larger drag force. The lift buffeting response of model series 2, similar to model series 1, also increases with B/H ratio, but the torsional response decreases with it. The calculated lift and torsional responses are in a similar trend with the results measured in reference [9]. Inspected from this table, it can be found that all of the calculated responses are smaller than the measured results and the differences are about 20%. The reason is that the calculated responses are based upon the buffeting theory that follows the quasi-steady assumption. The wind spectra and the span-wise correlation used in the calculation are not the same as those in the wind tunnel testing. Furthermore, the measured responses are transformed from the section model responses in which only two modes are considered. The transformation from the section model responses into the full bridge responses is simpli-

fied based upon many assumptions [9]. Therefore, the measured and the calculated results will not be the same and the discrepancy is reasonable.

The buffeting responses of the prototype bridge based upon the wind force coefficients and the flutter derivatives obtained in different flow fields are listed in Tables 9 and 10. The buffeting responses were calculated assuming that the bridge is subjected to the turbulent wind with the turbulence intensity in the range of 5% to 16%. In each case, the wind force coefficients and the flutter derivatives measured in smooth flow and in the corresponding turbulent flow were respectively used in the calculation. It clearly shows that the buffeting response of the bridge increases with turbulence. The calculated results based upon the wind force coefficients and the flutter derivatives measured in smooth flow are larger than those measured in the turbulent flow. Comparison between the calculated and measured buffeting responses indicates that all of the calculated responses are smaller than the measured responses. The reason is similar to those stated earlier. From the comparison, it can be also found that the calculated responses using the wind force coefficients and the flutter derivatives measured in smooth flow are closer to the measured responses than those measured in the turbulent flow. However, this does not imply using the aerodynamic coefficients measured in smooth flow in the calculation is more reasonable than those measured in the turbulent flow. This is because the measured buffeting responses, transformed from the section model response, are also the approximated values. From these results, we can conclude that the buffeting response, using the aerodynamic coefficients obtained in smooth flow, is more conservative.

7. Conclusions

Based on the wind tunnel test on several section models under various flow conditions, and the subsequent flutter and buffeting analysis, the following conclusions can be made:

(1) The bridge with the closed box girder deck has a significantly higher critical flutter wind speed than the plate girder deck. It makes the closed box girder a better aerodynamically stable deck shape.
(2) A flatter deck shape can improve bridge aerodynamic stability. This phenomenon is more effective for the plate girder deck than the closed box girder deck.
(3) The bridge has the better aerodynamic stability in a turbulent flow than the smooth flow field.
(4) Applying the wind force coefficients and flutter derivatives acquired from a section model test in smooth flow condition may result in more conservative buffeting estimation.

References

[1] Scanlan, R. H. and Tomko, J. J., "Airfoil and Bridge Deck Flutter Derivative," *J. Eng. Mech. Div.*, Vol. 97 (EM6), pp. 1717–1737 (1971).
[2] Bienkiewicz, B., "Wind Tunnel Study of Effects of Geometry Modification on Aerodynamics of a Cable Stayed Bridge Deck," *J. Wind Eng. Ind. Aerodyn.*, Vol. 26, pp. 325–339 (1987).
[3] Nagao, F., Utsunomiya, H., Oryu, T. and Manabe, S., "Aerodynamic Efficiency of Triangular Fairing on Box Girder Bridge," *J. Wind Eng. Ind. Aerodyn.*, Vol. 74, pp. 73–90 (1993).
[4] Matsumoto, M., Kbayashi, Y. and Shirato, H., "The Influence of Aerodynamic Derivative on Flutter," *J. Wind Eng. Ind. Aerodyn.*, Vol. 60, pp. 227–239 (1996).
[5] Matsumoto, M. and Abe, K., "Role of Coupled Derivative on Flutter Instabilities," *Wind Struct.*, Vol. 1, pp. 175–181 (1998).
[6] Scanlan, R. H. and Lin, W. H., "Effects of Turbulence on Bridge Flutter Derivatives," *J. Eng. Mech. Div.*, Vol. 104, pp. 719–733 (1978).
[7] Huston, D. R., Bosch, H. R. and Scanlan, R. H., "The Effect of Fairing and of Turbulence on the Flutter Derivatives of a Notably Unstable Bridge Deck," *J. Wind Eng. Ind. Aerodyn.*, Vol. 29, pp. 339–349 (1988).
[8] Wardlaw, R. L., Tanaka, H. and Utsunomiya, H., "Wind Tunnel Experiments on the Effects of Turbulence on the Aerodynamic Behavior of Bridge Road Decks," *J. Wind Eng. Ind. Aerodyn.*, Vol. 14, pp. 247–257 (1983).
[9] Lin, Y. Y., Cheng, C. M. and Lan, C. Y., "Effects of Deck's Width-to-depth Ratios and Turbulent Flows on the Aerodynamic Behaviors of Long-span Bridges,"

Wind Struct., Vol. 6(4), pp. 263–278 (2003).
[10] Lin, Y. Y., Cheng, C. M. and Lee, F. J., "Flutter and Buffeting Analysis of Long-span Bridges with Mode Coupling," *J. Chinese Ins. Civil Hydraulic Eng.*, Vol. 10, pp. 47–57 (1998).
[11] Simiu, E. and Scanlan, R. H., *Wind Effects on Structures*, 2nd ed., John Wiley & Sons, New York, NY, U.S.A. (1986).

Manuscript Received: Dec. 10, 2004
Revision Received: Jan. 26, 2005
Accepted: Feb. 21, 2005